Available online at www.sciencedirect.com
ScienceDirect
Comput. Methods Appl. Mech. Engrg. 326 (2017) 739–756
Computer methods in applied mechanics and engineering
www.elsevier.com/locate/cma

Global–Local ROM for the solution of parabolic problems with highly concentrated moving sources

Alejandro Cosimo[a], Alberto Cardona[a], Sergio Idelsohn[a,b,*]

[a] *CIMEC-Centro de Investigación de Métodos Computacionales (UNL/Conicet) Col. Ruta 168 s/n, Predio Conicet "Dr A. Cassano", 3000 Santa Fe, Argentina*

[b] *International Center for Numerical Methods in Engineering (CIMNE) and Institució Catalana de Recerca i Estudis Avançats (ICREA), Barcelona, Spain*

Received 11 April 2017; received in revised form 17 July 2017; accepted 23 August 2017
Available online 5 September 2017

Abstract

Problems characterised by steep moving gradients are challenging for any numerical technique and even more for the successful formulation of Reduced Order Models (ROMs). The aim of this work is to study the numerical solution of problems with steep moving gradients, by placing the focus on parabolic problems with highly concentrated moving sources. More specifically, a Global–Local scheme well-suited for reduction methods is formulated. With this Global–Local scheme, the local nature of the steep moving gradients is exploited by modelling the neighbourhood of the heat source with a moving local domain. This domain is coupled to the global domain without requiring any re-mesh and preserving the meshes of both domains during the whole simulation. Then, a ROM based on the Proper Orthogonal Decomposition (POD) technique is developed for the moving local domain. The proposed technique establishes a valid approach for tackling the *non-separability* of the space and time dimensions of these problems. In order to assess the numerical performance of the proposed numerical techniques, several evaluation tests are performed.

Keywords: Global–Local schemes; Reduced Order Models; Steep moving gradients; Parabolic problems; Moving heat source

1. Introduction

Numerical simulation of complex phenomena in engineering usually helps to decrease the number of experimental studies to be made before final design decisions are taken. In some cases, such as when a wide range of parameters of the process need to be studied, the number of simulations to be performed can be quite high. This process may require too much time, what makes it unaffordable in the development of a given product. The aim of this work is to study problems with moving gradients, such as those produced by a highly concentrated moving source, which

* Corresponding author at: International Center for Numerical Methods in Engineering (CIMNE) and Institució Catalana de Recerca i Estudis Avançats (ICREA), Barcelona, Spain
E-mail addresses: acosimo@cimec.unl.edu.ar (A. Cosimo), acardona@cimec.unl.edu.ar (A. Cardona), sergio@cimne.upc.edu (S. Idelsohn).

http://dx.doi.org/10.1016/j.cma.2017.08.036
0045-7825/

usually demand large simulation times due to the fact that both small time steps and fine mesh sizes are required for the simulation. The computational time will be reduced in this context with the development of special Reduced Order Models.

Focus in this work will be placed on parabolic problems with highly concentrated moving sources. A naive approach to deal with this kind of problems is to refine the mesh as much as needed in regions of the domain which are in the vicinity of the trajectory to be followed by the source. Clearly, this is not a practical solution as the computational cost does not decrease considerably. One alternative is to adaptively refine the mesh in the surroundings of the moving source [1]. Despite the fact that this option will decrease the problem size, for certain applications this will not be enough mainly because the number of degrees of freedom could still be quite large and the topology of the mesh will be constantly changing. It must be noted that both methodologies are not well adapted to the formulation of ROMs. In the case of adaptive mesh refinement, the fact that the mesh changes constantly is not a desirable feature in most ROM techniques. In the alternative of refining the mesh in the vicinity of the trajectory followed by the source, a ROM technique can be classically applied. However, it is not possible to introduce the trajectory of the source as a parameter of the ROM and, as shown in [2] for the case of a POD-based ROM, the number of modes can be quite large when a Lagrangian frame of reference is adopted. This problem is sometimes attributed to the lack of *separability* of the space and time dimensions. A simple benchmark has been proposed by S. Idelsohn, consisting of a one-dimensional transient heat conduction problem with a moving source, which is quite difficult to be solved by reduction methods despite its apparent simplicity. In a recent work of Allier et al. [3], a new strategy based on the Proper Generalised Decomposition (PGD) method is proposed for dealing successfully with the space–time separability issue.

Another alternative is to rely on formulations which exploit the local nature of the steep moving gradients. Two approaches can be mentioned. One option is to describe the local features of the problem by enriching the Finite Element (FE) space. The work of Canales et al. [4] addresses this problem by using the Generalised Finite Element Method (GFEM). They propose to enrich the solution in the neighbourhood of the heat source with only one enrichment function. This enrichment is the parametric solution to a local problem which takes the temperature of the surrounding as boundary conditions. In order to efficiently deal with the computation of these parametric solutions, they adopt the PGD method. A detail of this methodology is that the enrichment function is the solution to a steady state problem, therefore the resulting enrichment will not describe correctly the non-stationary regime of the problem. An alternative related to this technique, however more expensive, is the Global–Local GFEM (GFEM^{gl}) [5,6] where a time dependent enrichment function is determined from the *on-line* solution of a local problem, without generally using a reduction technique. Canales et al. mention that building time dependent enrichment functions in a Global–Local approach is possible, however expensive. Furthermore, they remark that a POD-based approach for computing the enrichment function would have the drawback that the number of modes can be quite large, and that those modes will not be effective to model other problems than those solved during the training phase.

The other approach to exploit the local nature of the steep moving gradients also involves the solution of a global and a local problem, but without using any enrichment. The idea of adopting local domains for describing local features of the problem is wide-spread and has multiple forms, such as for example, the Chimera methodologies [7], the Schwarz-based techniques [8] and the Arlequin method [9]. Our aim is to develop a numerical technique which is able to handle in a non-iterative manner the gluing of a *moving* local domain to the global domain, where the mesh size of the local domain can be much smaller than that of the global domain. It should be noted that for the described situation, compatibility conditions between the local and global domains cannot be imposed strongly. Therefore, the use of Lagrange multipliers raises as the natural solution. Adopting this perspective, Christophe et al. [10,11] analysed an eddy current non-destructive testing problem, where a moving domain needs to be coupled to a global fixed domain. In order to deal with that issue, they made in the global domain an artificial hole comprised by the elements completely overlapped by the local domain. Then, the transmission conditions were imposed on the boundary of the moving domain *and* on the (*changing*) boundary determined by the artificial hole made in the global domain. It must be noted that imposing the transmission conditions on the boundary determined by the artificial hole makes necessary to define a Lagrange multipliers field on that boundary. This is an undesirable feature for the formulation of ROMs, due to the fact that the involved boundary is constantly changing. Another Global–Local strategy is proposed by Zeng et al. [12], where a local domain moves at "discrete jumps" in such a way that the boundary of the local domain conforms to the elements' boundary of the mesh of the global domain, something we would like to avoid. It is also remarked that there exists another related paradigm in which a global model is modified locally by another submodel in a *non-intrusive* manner as presented, for instance, by Gendre et al. [13]. Due to the fact that this kind of technique is iterative, it is not adopted as paradigm in this work.

In this paper we formulate a Global–Local scheme well-suited to reduction methods without using an enrichment technique. More specifically, the resulting methodology must enable the reduction of the local problem by the use of POD methodologies. In order to achieve this, we begin with the formulation of a Global–Local scheme which is similar to the approach presented by Christophe et al. [10,11]. However, in our proposal, we also make an artificial hole in the global domain without any remeshing involved, but that hole exactly coincides with the overlapped region by the local domain. Elements of the global domain partially intersected by the local domain will contribute only with the region of the element which is not overlapped by the local domain. This allows us to impose the transmission conditions only on the boundary of the local domain, which makes the resulting methodology better suited to POD-based reduction methodologies. Several other aspects specific to transient problems with moving local domains are carefully studied. They concern, for instance, the projection of the information from the previous time step to the current time step and which compatibility constraint is best to impose.

The paper is organised as follows. Section 2 states the mathematical setting of the problem to be studied and it introduces two formulations for dealing with a steep moving gradient within a moving local domain which is coupled to a global domain. In Section 3, a Reduced Order Model which exploits the *compressibility* of the solution on the moving local domain is devised. In order to assess the numerical performance of the proposed numerical techniques, evaluation tests are performed in Section 4. These tests are organised in two groups. On one group, the performance of the introduced Global–Local schemes is analysed, and, on the other group, the behaviour of the proposed Reduced Order Model for the local domain is studied. Finally, Section 5 gives the conclusions and future work.

2. Mathematical setting and formulation of a Global–Local Scheme

We analyse problems with steep moving gradients by adopting a Global–Local scheme, in which the neighbourhood of the moving gradient is described by a moving local domain with a fine mesh and in which the global domain is described by a coarse mesh. In order to introduce the proposed numerical scheme, we restrict our study to transient heat conduction *linear* problems with a concentrated moving heat source. This is not a limitation as it will become evident from the presented examples, where the potential to deal with non-linear problems and other than transient heat conduction will be recognised. The equations governing the physical problem to be studied are:

$$\frac{\partial u}{\partial t} - k\Delta u = Q, \quad \text{for } x \in \Omega \text{ and } t \in [0, T], \tag{1}$$

with appropriate boundary and initial conditions, where Ω denotes the analysis domain, T is the end of the time interval, $u(x, t)$ is the temperature field and $Q(x, t)$ is the heat source which is given by

$$Q(x, t) = Q_m e^{-\frac{\xi \cdot \xi}{\sigma^2}}, \tag{2}$$

where $\xi = x - x_0 - vt$, x_0 is the initial position, v is the velocity, Q_m is a scalar parameter, and σ is a parameter which controls how concentrated is the heat source.

Making the assumption of high gradients around the moving heat source and that they smooth out as the source travels, we propose to describe the domain of analysis using a very coarse global mesh and the behaviour in the neighbourhood of the heat source by a moving local domain with a very fine mesh. In order to understand the basic algorithm for gluing the local and global domains, the case in which the local domain is fixed with the heat source moving inside its support is first analysed. Then, the case in which the local domain moves following the heat source is studied.

2.1. Fixed local domain

Let $\Omega_c \equiv \Omega$ and Ω_f denote the global and local domains, respectively (see Fig. 1a). A *non-overlapping* domain decomposition of the analysis domain Ω can be built by removing the region which overlaps with the local domain from the global domain, resulting in $\hat{\Omega}_c = \Omega_c - \Omega_c \cap \Omega_f$. Then, the domains $\hat{\Omega}_c$ and Ω_f form a *non-overlapping decomposition* of Ω, from which problem (1) can be re-stated as find $u^c \in \hat{\Omega}_c$ and $u^f \in \Omega_f$ subject to the transmission conditions $u^c - u^f = 0$ and $\nabla u^c \cdot n + \nabla u^f \cdot n = 0$ on the interface Γ determined by both domains, where n denotes

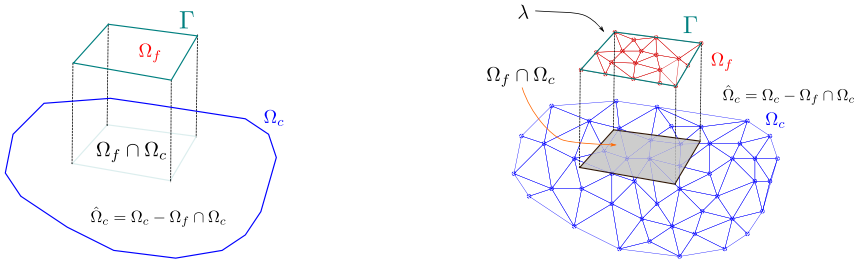

Fig. 1. (a) Definition of the global and local domains. (b) Both domains are independently meshed. The heat source is only modelled on the local domain.

the outward normal of the local domain at the interface Γ. Variationally, this writes: Find $u^c \in \mathcal{H}^1_{\hat{\Omega}_c}$, $u^f \in \mathcal{H}^1_{\Omega_f}$ and $\lambda \in \mathcal{H}^{-1/2}_{\Gamma}$ such that

$$m_c(\delta u^c, u^c) + k_c(\delta u^c, u^c) + c(\delta u^c, \lambda) = q_c, \qquad \forall \delta u^c \in \mathcal{H}^1_{\hat{\Omega}_c}, \tag{3}$$

$$m_f(\delta u^f, u^f) + k_f(\delta u^f, u^f) - c(\delta u^f, \lambda) = (\delta u^f, Q), \qquad \forall \delta u^f \in \mathcal{H}^1_{\Omega_f}, \tag{4}$$

$$c(\delta\lambda, u^c - u^f) = 0, \qquad \forall \delta\lambda \in \mathcal{H}^{-1/2}_{\Gamma}, \tag{5}$$

where

$$m_i(v,u) = \int_{\Omega_i} v \frac{\partial u}{\partial t}\, d\Omega\,, \qquad k_i(v,u) = \int_{\Omega_i} \nabla v \cdot k \nabla u\, d\Omega\,, \qquad c(v,\lambda) = \int_{\Gamma} v\lambda\, d\Gamma\,,$$

$$(v, Q) = \int_{\Omega_f} vQ\, d\Omega,$$

for $i = [c, f]$, and the term q_c denotes the contribution from boundary conditions in the global domain. It should be noted that the moving heat source Q is modelled only in the local domain Ω_f.

Remark. In the discretisation of the previous formulation, the space for the Lagrange multipliers will be restricted to discrete subsets of L^2_Γ as it is usually done in Mortar methods [14]. Note that, on the continuous level, integrals are not defined for elements of $\mathcal{H}^{-1/2}_{\Gamma}$ and duality pairings should be used instead. For the sake of readability, integrals are adopted for the terms involving the compatibility conditions, which in fact make sense at the discrete level.

The discretisation of the variational problem is introduced next. Linear finite elements will be adopted for the discretisation of the temperature field, and the Lagrange multipliers field will be defined using linear shape functions over the boundary of the fine mesh. In the case of two-dimensional problems, linear triangular elements are used. Three-dimensional problems will not be addressed in this work, nonetheless the ideas presented here extend straightforwardly to that case.

The domains Ω_c and Ω_f are independently meshed for the discretisation of the variational problem, as shown in Fig. 1b. Therefore, in general, the boundary of the local domain will not conform to the elements boundary of the global domain mesh. This situation complicates the definition of the domain $\hat{\Omega}_c$ if re-meshing must be avoided as in the present work. In order to solve this problem, the unknown u^c will be discretised using as support the mesh of domain Ω_c. Therefore, all degrees of freedom (DOFs) belonging to the global domain Ω_c are considered as unknowns of the problem. However, the domain involved in the variational formulation is $\hat{\Omega}_c$. In order to recover $\hat{\Omega}_c$, an artificial hole is made in domain Ω_c at its intersection with the local domain. This involves classifying which DOFs of the global domain will take part of the computations and which ones not. The first group of DOFs will be referred to as *active* DOFs and the other group will be referred to as *inactive* DOFs. As it will be observed, inactive DOFs will take part of the computations, but with a special treatment. The classification of DOFs is performed as follows: DOFs belonging only to elements completely intersected by the local domain are classified as inactive DOFs. The rest of DOFs, which belong to elements which are not intersected by the local domain or which are *partially* intersected

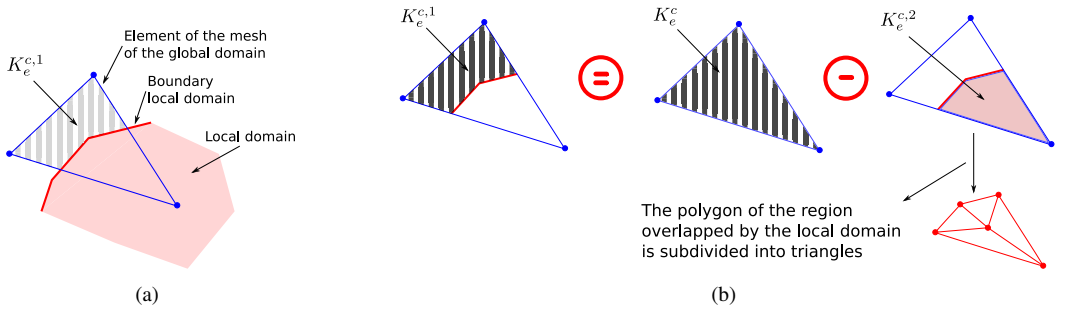

Fig. 2. (a) Triangle of the mesh of the global domain partially intersected by the local domain. (b) Procedure followed for the computation of the contribution of partially intersected elements to the element stiffness matrix.

elements by the local domain, are classified as active DOFs. The columns and rows corresponding to DOFs classified as inactive DOFs in the associated system of equations are zeroed and the related diagonal entries are set to one. This procedure, together with a correct computation of the involved integrals which will be introduced next, is what we understand by *numerically cutting* the domain Ω_c.

As said before, an important aspect of *numerically cutting* domain Ω_c concerns the correct computation of integrals defined over the domain $\hat{\Omega}_c$. The contributions of elements whose DOFs are all active do not represent any complication, because the involved elements are not overlapped by the local domain. The problematic elements are those *partially* intersected by the local domain as shown in Fig. 2a. In order to correctly compute these contributions, the integration region is limited to the region of the element which is not overlapped by the local domain. In this way, we avoid adding twice the contribution of the integrals in the regions of elements of the global domain intersected by the local domain. In order to understand the details of the integration of intersected elements, consider the situation presented by Fig. 2b where an element e from the global domain is *partially* intersected by the local domain. The contribution of this element to the stiffness matrix is denoted in the figure as $K_e^{c,1}$, where it is clear that only the region that is not overlapped contributes. For its computation, the polygon of the overlapped region is first determined. Then, a triangulation is built with the polygon and its centroid, which is used for computing the stiffness of the element corresponding to the overlapped area, $K_e^{c,2}$. Finally, $K_e^{c,1}$ is obtained by subtracting from the stiffness of the element K_e^c the stiffness of the overlapped region, *i.e.*, $K_e^{c,1} = K_e^c - K_e^{c,2}$.

Remark. It should be noted that the size of matrix $K_e^{c,1}$ is 3×3, that is, every node contributes to the element matrix regardless if one or more nodes of the element are in the region overlapped by the local domain. The only thing which is redefined in order to compute $K_e^{c,1}$ is the integration region of the element. The definition of the involved shape functions is not modified, they are defined in terms of the position of the element nodes.

Another detail of the discretisation of the variational formulation is how to discretise the terms involved by the restriction, Eq. (5). Let ϕ_i, N_j^c and N_j^f be the shape functions used to interpolate λ, u^c and u^f, respectively, such that

$$\lambda(x) = \sum_{i=1}^{n_\lambda} \phi_i(x)\underline{\lambda}_i \equiv \phi^T \underline{\lambda}\,, \qquad u^c(x,t_n) = \sum_{j=1}^{n_c} N_j^c(x)\underline{u}_{n,j}^c \equiv N^{c,T}\underline{u}_n^c\,,$$

$$u^f(x,t_n) = \sum_{j=1}^{n_f} N_j^f(x)\underline{u}_{n,j}^f \equiv N^{f,T}\underline{u}_n^f,$$

where n_λ, n_c and n_f are the number of DOFs for the Lagrange multipliers and for the temperature field on the global and the local domain, respectively. Let also $\chi : \Gamma \to \Omega^c$ be a mapping from Γ to the domain Ω^c, such that it satisfies that $\int_\Gamma \delta\lambda \left[u^c\left(\chi(x)\right) - u^f\left(x\right)\right] d\Gamma = 0$, where $u^c\left(\chi(x)\right)$ can be interpreted as the projection of $u^c \in \Omega^c$ on Γ. Then, the discrete version of Eq. (5) at time t_n is given by

$$B^c\underline{u}_n^c + B^f\underline{u}_n^f = 0,$$

where the entries of matrices B^c and B^f are given by

$$B^c_{i,j} = -\int_\Gamma \phi_i (N^c_j \circ \chi)\, d\Gamma, \qquad B^f_{i,j} = \int_\Gamma \phi_i N^f_j \, d\Gamma.$$

Remark. The adopted discretisation for the Lagrange multipliers is based on the theory of Mortar methods [15]. If the DOFs at the boundary of the local domain are considered to be the slave DOFs, then a suitable choice for the discretisation of the Lagrange multipliers is given by the trace of the discrete version of the solution space for the temperature field on the local domain.

Therefore, making use of the introduced concepts and discretising in time with a θ-method, the variational formulation results in the following system of equations

$$\begin{bmatrix} M^c + \theta \Delta t K^c & 0 & B^{c,T} \\ 0 & M^f + \theta \Delta t K^f & B^{f,T} \\ B^c & B^f & 0 \end{bmatrix} \begin{bmatrix} \underline{u}^c_n \\ \underline{u}^f_n \\ \underline{\lambda} \end{bmatrix} = \begin{bmatrix} \theta \Delta t q^c_n + \beta \Delta t q^c_{n-1} + (M^c - \beta \Delta t K^c)\underline{u}^c_{n-1} \\ \theta \Delta t q^f_n + \beta \Delta t q^f_{n-1} + (M^f - \beta \Delta t K^f)\underline{u}^f_{n-1} \\ 0 \end{bmatrix}, \tag{6}$$

where $\beta = 1 - \theta$, and M^i and K^i are the mass matrix and the stiffness matrix corresponding to domain i, respectively.

2.2. Moving local domain

In the previous section, we introduced a Global–Local methodology which is able to couple a global domain and a local domain which describes some local feature such as a moving heat source which generates steep moving gradients. It was assumed that the local domain is fixed and that the heat source moves within its support. Here, we extend the introduced Global–Local scheme to a local domain with a mesh with fixed topology which moves following the heat source. Different variants can be considered in this case, which are described next.

A straightforward solution is to use the discrete formulation introduced before, Eq. (6). However, in this case the movement of the local domain introduces a new issue: What is the expression of the solution at the previous time step, i.e. u^c_{n-1} and u^f_{n-1}, when the local domain moves and adopts the configuration corresponding to the current time step t_n? An answer to this question is to project the solution at the previous time step to the configuration adopted by the local domain. It must be observed that two projections are needed, one for building u^c_{n-1} and the other for building u^f_{n-1}. In order to understand this, note that the solution at the global domain u^c_{n-1}, before the local domain moves, is defined only on nodes lying on the region not overlapped by the local domain. When that domain moves in the next time step, some nodes that were in the overlapped region at the previous time step will not be there anymore. This makes it necessary to define a state at the previous time step for those nodes. This can be done by projecting the information from the local domain in the previous configuration to the global domain. Something similar needs to be done for the local domain. This procedure can be observed in Fig. 3 when a collocation method is used in a one-dimensional case.

It must be kept in mind that some artificial diffusion will be introduced when projections are performed using a collocation methodology. Other less diffusive approaches can be used at the expense of increasing the computational cost, such as, for example, a mortar-like projection which conserves energy [16]. In the present paper, the projections are performed by collocation, in order to save computational time.

The fact that the local domain moves attached to the heat source can be exploited in order to avoid one of the projections mentioned before. The movement of this domain can be described by adopting an Arbitrary Lagrangian Eulerian (ALE) description [17]. A fundamental advantage of this description is that the need of projecting information in order to express u^f_{n-1} in the configuration adopted by the local domain at time t_n is not needed anymore. Then, the

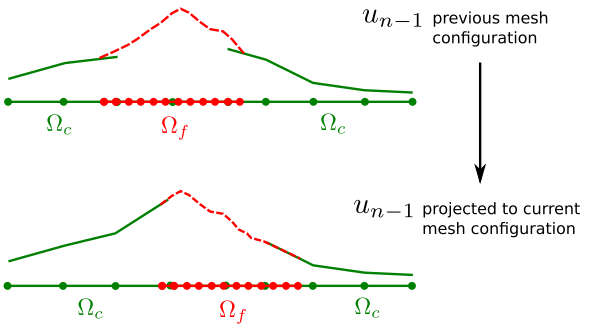

Fig. 3. Projecting previous time step to the new mesh configuration using collocation.

discrete formulation of the problem is given by the following set of equations

$$\begin{bmatrix} M^c + \theta \Delta t K^c & 0 & B^{c,T} \\ 0 & M^f + \theta \Delta t (K^f - A^f) & B^{f,T} \\ B^c & B^f & 0 \end{bmatrix} \begin{bmatrix} \underline{u}_n^c \\ \underline{u}_n^f \\ \underline{\lambda} \end{bmatrix} = \begin{bmatrix} \Delta t(\theta q_n^c + \beta q_{n-1}^c) + (M^c - \beta \Delta t K^c)\underline{u}_{n-1}^c \\ \Delta t(\theta q_n^f + \beta q_{n-1}^f) + (M^f + \beta \Delta t [A^f - K^f])\underline{u}_{n-1}^f \\ 0 \end{bmatrix}, \tag{7}$$

where A^f is the advection matrix.

Remark. The problem in the local domain is given by a time dependent advective–diffusive equation. Therefore, a stabilisation term must be used for Péclet numbers larger than 1. The stabilisation of the formulation is considered out of the scope of this work, as it is assumed that the local domain can be refined as much as needed in order to avoid high Péclet numbers. The refinement of the local domain is not a problem, because it is the domain to be reduced. However, if this is not possible, further study on a stabilisation technique must be accomplished. It should be noted that the driving force of this problem is the heat source, from which it could be a real problem to determine a stabilisation parameter which does not introduce too much diffusivity.

In the previous formulation, compatibility of the temperature field was imposed at the interface between domains $\hat{\Omega}_c$ and Ω_f. Another option, whose advantage will be discussed in Section 4, is to impose compatibility of the *material* time derivative of temperature at the portion $\hat{\Gamma}$ of the interface Γ satisfying $v \cdot n < 0$, with n denoting the outward-normal of the interface Γ. In the portion $\Gamma - \hat{\Gamma}$, compatibility of the temperature field is imposed. That is, we propose to impose the restrictions

$$\dot{u}^c = \dot{u}^f - v \cdot \nabla u^f, \quad \text{on } \hat{\Gamma} \tag{8}$$

$$u^c = u^f, \quad \text{on } \Gamma - \hat{\Gamma}. \tag{9}$$

Let us analyse in detail the case of imposing as compatibility constraint Eq. (8). It should be observed that the *continuous* variational formulation (3)–(5) can be modified by replacing Eq. (5) by

$$d(\delta\lambda, u^c, u^f, \dot{u}^c, \dot{u}^f) = \int_{\hat{\Gamma}} \delta\lambda(\dot{u}^c - \dot{u}^f + v \cdot \nabla u^f)\, d\Gamma + \int_{\Gamma - \hat{\Gamma}} \delta\lambda(u^c - u^f)\, d\Gamma = 0. \tag{10}$$

However, it must be noted that the terms $c(\delta u^i, \lambda)$ of Eqs. (3), (4) for $i = [c, f]$ are not modified. This ensures that the following transmission conditions are imposed on Γ

$$\begin{aligned} u^c &= u^f, && \text{on } \Gamma - \hat{\Gamma} \\ \dot{u}^c &= \dot{u}^f - v \cdot \nabla u^f, && \text{on } \hat{\Gamma} \\ k\nabla u^c \cdot n &= -k\nabla u^f \cdot n, && \text{on } \Gamma. \end{aligned}$$

The first term of Eq. (10) is discretised in time using the θ-method, resulting in

$$\int_{\hat{\Gamma}} \delta\mu(u_n^f - \theta\Delta t v\cdot\nabla u_n^f - u_n^c)\,d\Gamma = \int_{\hat{\Gamma}} \delta\mu(u_{n-1}^f + \beta\Delta t v\cdot\nabla u_{n-1}^f - u_{n-1}^c)\,d\Gamma\,. \tag{11}$$

Then, the discrete set of equations of this alternative are given by

$$\begin{bmatrix} M^c + \theta\Delta t K^c & 0 & B^{c,T} \\ 0 & M^f + \theta\Delta t(K^f - A^f) & B^{f,T} \\ B^c & B^f + \theta\bar{B}^f & 0 \end{bmatrix} \begin{bmatrix} \underline{u}_n^c \\ \underline{u}_n^f \\ \underline{\lambda} \end{bmatrix} = \begin{bmatrix} \Delta t(\theta q_n^c + \beta q_{n-1}^c) + (M^c - \beta\Delta t K^c)\underline{u}_{n-1}^c \\ \Delta t(\theta q_n^f + \beta q_{n-1}^f) + (M^f + \beta\Delta t[A^f - K^f])\underline{u}_{n-1}^f \\ \hat{B}^c\underline{u}_{n-1}^c + (\hat{B}^f - \beta\bar{B}^f)\underline{u}_{n-1}^f \end{bmatrix}, \tag{12}$$

where the entries of matrices $\bar{B}^f$, $\hat{B}^c$ and $\hat{B}^f$ are given by

$$\bar{B}_{i,j}^f = -\Delta t\int_{\hat{\Gamma}} \phi_i v\cdot\nabla N_j^f\,d\Gamma\,, \qquad \hat{B}_{i,j}^c = -\int_{\hat{\Gamma}} \phi_i(N_j^c\circ\chi)\,d\Gamma\,, \qquad \hat{B}_{i,j}^f = \int_{\hat{\Gamma}} \phi_i N_j^f\,d\Gamma.$$

3. Development of a reduced order model for the moving local domain

The formulation of an *a posteriori* ROM technique based on the POD method is now proposed, to deal with the dimensionality of problems with steep moving gradients. POD-based ROMs are *a posteriori* techniques, because the construction of the ROM requires to know first the High-Fidelity (HF) solution to a set of training problems [18]. Generally, two reduction steps are needed for a ROM to be successful in reducing computation times. In the first reduction, the dimension of the discrete versions of the test and trial spaces is tackled. Nevertheless, for non-linear problems, the cost of assembling the non-linear forces and the tangent matrix can be significant, making necessary to perform a second reduction known as hyper-reduction [19,20]. In the present work, attention will be paid to the first reduction step, due to the fact that the main complication in the reduction of problems with steep moving gradients is in this step. The hyper-reduction of this ROM will be object of study of a future work. However, in principle, standard hyper-reduction techniques [2,20] should work once it is known how to successfully reduce the test and trial spaces of the involved problem.

Cosimo et al. [2] showed that POD-based ROMs perform well for problems with steep moving gradients as those present in welding applications, provided the frame of reference moves attached to the moving gradient. It was observed that the number of POD modes needed for describing the unknowns is quite small. In other words, the resulting description is characterised by a set of snapshots which display a high *compressibility*.

The first reduction step of a POD-based ROM consists in initially building a set of *snapshots* of the solution of the training problems [21]. Then, the Singular Value Decomposition [22] of the snapshots matrix is computed, taking the left singular vectors (also in this paper referred to as *POD modes*) as a reduced basis which captures the response of the system under study with a small number n_r of POD modes. In order for the ROM to be successful, n_r must be much smaller than the number of DOFs N of the HF model, that is $n_r \ll N$. In what follows, we will not deal with essential boundary conditions. However, for the case of problems involving non-homogeneous essential boundary conditions, a slightly different procedure must be applied in order to correctly compute POD modes as explained in [23].

The formulation of a POD-based ROM is investigated for the reduction of the problem of the local domain. Two formulations were introduced in the previous section for dealing with moving local domains in the context of a Global–Local methodology. Both developed alternatives share the common feature that the local domain moves attached to the heat source, from which they can be expected to give a set of snapshots with a high *compressibility*. This investigation will focus on the alternative where the material time derivative of temperature is imposed as compatibility constraint. Therefore, the developed ROM is based on Eq. (12) which is re-written for conciseness as

$$\begin{bmatrix} G^c & 0 & B^{c,T} \\ 0 & G^f & B^{f,T} \\ B^c & \tilde{B}^f & 0 \end{bmatrix} \begin{bmatrix} \underline{u}_n^c \\ \underline{u}_n^f \\ \underline{\lambda} \end{bmatrix} = \begin{bmatrix} g_1 \\ g_2 \\ g_3 \end{bmatrix}, \tag{13}$$

where

$$G^c = M^c + \theta \Delta t K^c, \qquad G^f = M^f + \theta \Delta t (K^f - A^f),$$
$$g_1 = \Delta t(\theta q_n^c + \beta q_{n-1}^c) + (M^c - \beta \Delta t K^c)\underline{u}_{n-1}^c, \qquad g_3 = \hat{B}^c \underline{u}_{n-1}^c + (\hat{B}^f - \beta \bar{B}^f)\underline{u}_{n-1}^f,$$
$$g_2 = \Delta t(\theta q_n^f + \beta q_{n-1}^f) + (M^f + \beta \Delta t[A^f - K^f])\underline{u}_{n-1}^f, \qquad \tilde{B}^f = B^f + \theta \bar{B}^f.$$

In what follows, the Lagrange multipliers and the temperature field at the local domain are separately reduced (see [23] for an extended discussion on the reduction of Lagrange multipliers). Once the POD modes are computed from the snapshots of each quantity, the trial solution functions corresponding to the Lagrange multipliers and to the temperature field, respectively denoted by λ and u^f, can be expressed as

$$\lambda \approx \phi^T Y \underline{b}, \qquad u^f \approx N^{f,T} X \underline{a}_n,$$

where Y and X are, respectively, the POD modes for the Lagrange multipliers and the temperature field, with their corresponding coefficients $\underline{b}$ and $\underline{a}_n$. Then, the Reduced Order Model for the problem under study takes the expression

$$\begin{bmatrix} G^c & 0 & B^{c,T} Y \\ 0 & X^T G^f X & X^T B^{f,T} Y \\ Y^T B^c & Y^T \tilde{B}^f X & 0 \end{bmatrix} \begin{bmatrix} \underline{u}_n^c \\ \underline{a}_n \\ \underline{b} \end{bmatrix} = \begin{bmatrix} g_1 \\ X^T g_2 \\ Y^T g_3 \end{bmatrix}. \tag{14}$$

It should be noted that a Bubnov–Galerkin projection was used, which is valid for problems with a Symmetric Positive Definite (SPD) Jacobian. If the Jacobian of the problem is non-symmetric, a Petrov–Galerkin projection should be adopted as proposed in [24]. In the case of the formulation for the local domain and also when dealing with non-linear transient heat conduction, the Jacobian is non-symmetric. Despite this fact, the non-symmetry is not as large as in fluid mechanics problems and a Bubnov–Galerkin projection gives good results for the present case as shown in [2].

3.1. Introduced sources of error and involved operations

In order to estimate the cost of the proposed methodology and the introduced sources of errors, each simplifying hypothesis is analysed along with the algorithms used to implement the corresponding model.

The most expensive, although the most accurate, option for numerically solving a problem with a moving concentrated heat source, is to refine everywhere, *i.e.* to adopt a global domain with a very fine mesh. However, the cost of this solution would be extremely high in terms of the number of involved DOFs. Therefore, a Global–Local scheme is proposed in which only the local domain has a fine mesh. The introduced sources of error will be the coarse description of the global domain, despite the fact that it is assumed that the solution varies rapidly only inside the local domain, and the projection by collocation used for the construction of u_{n-1}^c at time t_n. An additional source of error can be introduced if a stabilisation scheme is adopted for the local domain. Despite the introduced sources of error, the number of DOFs will be greatly reduced for some problems with the Global–Local scheme, and thus the computational cost. It should be observed that the cost of computing the intersections needed for numerically cutting Ω^c and the projection for building u_{n-1}^c, operations which are analysed next, do not have a high contribution to the total cost.

The local domain is assumed to be of rectangular shape (note that this assumption does not introduce any limitation) in order to efficiently compute the polygon of intersection between the local domain and elements of the global domain. Therefore, the intersections are computed between elements of the global domain and the rectangle representing the local domain, referred to in what follows as the *bounding rectangle*. Then, the computation of the intersections involves the following steps. First, find which elements of the global domain are intersected by the bounding rectangle. This is quite fast, because it involves finding out if the nodes of a given element are within the bounding rectangle. This operation can be done very efficiently by making use of spatial ordering techniques, such as quad-trees in the global domain. In a second step, the polygon of intersection is computed only for the elements of the global domain which were intersected by the bounding rectangle. The algorithm for computing such intersection is described elsewhere [25]. Therefore, it is clear that the cost of computing the intersections between elements is restricted to very few elements of the mesh of the global domain. Then, if the largest side of the local domain has a length of rh_c, with h_c being the mesh size of the global domain and r a positive constant, only $O(r)$ intersections need to be computed. It should be noted that r is in general quite small, because it is assumed that the mesh of the global domain is coarse.

In order to build u^c_{n-1} at time t_n, a projection by collocation is involved. Basically, this operation consists in finding the nodes of the global mesh that lie in elements of the mesh of the local domain corresponding to its configuration at time t_{n-1}. Once a node is found to lie in the local domain, the temperature field is accordingly interpolated with the values of the local domain. Therefore, the most expensive operation is to find the element of the local domain over which a given node of the global domain is projected. However, this operation is cheap. First, it is checked if a point is inside the bounding rectangle of the local domain. In such case, the search for the element over which it projects begins. Nonetheless, this can be done quite fast if *temporal coherence* is exploited, *i.e.* by taking into account that a given node is probably lying in the neighbourhood of the element in which it lied in the previous time step. This is implemented, for instance, by saving for each node of the global domain the number of the element in which it lied at time t_{n-1} and to use it in the next time step as the initial element where to start the search. This can be further improved by using spatial ordering data structures and by noting that the projection is only needed in regions of the global domain that were below the local domain at time t_{n-1} but which are not below it at the current time t_n.

The other improvement that is proposed in this paper is to reduce the problem of the local domain. Here, the gain is obvious as the number of DOFs can be greatly reduced, of course at the expense of introducing another source of error.

4. Evaluation tests

Several evaluation tests are performed in this section in order to assess the numerical performance of the proposed numerical techniques. These tests are organised in two groups. In one group, the performance of the introduced Global–Local schemes is analysed, and, in the other group, the behaviour of the proposed Reduced Order Model for the local domain is studied. In order to evaluate the performance of the Global–Local scheme, the error E at time t_n between a reference solution u_r and the numerical solution u is measured as

$$E(t_n) = \frac{\|u(x, t_n) - u_{ref}(x, t_n)\|}{\|u_{ref}(x, t_n)\|}, \tag{15}$$

where $\|\cdot\|$ is the L_2 norm of $\cdot$. The reference solution u_r is the semi-analytic solution of the problem obtained by using the corresponding Green function [26]. Due to the fact that the domain of analysis is discretised into a global and a local domain, a reference mesh is built in order to compare functions defined on the analysis domain. Then, the function to be studied is evaluated over this reference mesh. That is, the temperature field u is built by projecting $\underline{u}^c$ and $\underline{u}^f$ to the reference mesh. In the examples which follow, the projection is performed by *collocation* [16]. In all the examples presented below, a θ-integration scheme with $\theta = 2/3$ is used, and, if nothing is said, the error is measured at the end of the time interval. Additionally, the lumped mass matrix is adopted.

4.1. Numerical performance evaluation of the Global–Local scheme

4.1.1. Test 1: fixed local domain

A 1D example with a fixed local domain and a moving heat source is presented. The domain of analysis is a bar 720 units long, the material conductivity is 2, the velocity of the heat source is 0.9 which is initially positioned at $x = 250$. The local domain origin is set at 170 units from the origin of the coarse domain and it has a length of 330 units. The rest of the heat source parameters are set to $\sigma = 10$ and $Q_m = 100$. Homogeneous Neumann boundary conditions and an initial temperature equal to zero are used. The simulated time interval is $t \in [0, 223.5]$. Convergence in space is studied using a mesh of 600 equally-spaced points as reference mesh and a time step of 0.15. The obtained results can be observed in Fig. 4, where not only the results for equal mesh sizes for the global and local domains are shown, but also for a global domain with a mesh of 20 elements. These options are respectively denoted in the figure by *"Global–Local"* and by *"Global–Local coarse"*. From these results, it can be concluded that the Global–Local approach does not introduce any source of error when compared to the convergence of the classical FEM solution. However, it should be kept in mind that the path followed by the heat source is fully covered by the support of the local domain which does not move.

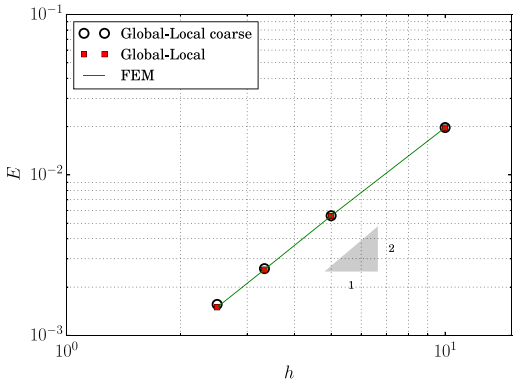

Fig. 4. Convergence in space for 1D test where the local domain does not move and the heat source trajectory is fully covered by its support.

4.1.2. Test 2: equal mesh sizes for both domains

In this test, a local domain which moves following the heat source, with equal mesh sizes for the global and local domains, is studied. The local domain describes only a portion of the path followed by the heat source and not the complete path as in Test 1. In this case, one and two dimensional studies are performed. The 1D study is similar to that of Section 4.1.1, with the difference that the local domain has a length of 120 units with its centre coincident with that of the heat source. The origin of this domain at the initial time t_0 is located at 190 units with respect to the origin of the coarse domain.

The domain of analysis of the two dimensional study is a rectangle of 500 $\times$ 200 units, the material conductivity is 2, the velocity of the heat source is [0.9, 0] which is initially positioned at $x = (120, 100)$. The local domain, whose size is 100 $\times$ 100 units, has at every time step its centre coincident with that of the heat source. The rest of the heat source parameters are set to $\sigma = 10$ and $Q_m = 100$. Homogeneous Neumann boundary conditions and an initial temperature equal to zero are imposed. The simulated time interval is $t \in [0, 292.5]$. The reference mesh size is equal to the finest tested mesh for the local domain and a time step of 7.5 is used.

Convergence in space is studied. The obtained results can be observed in Fig. 5a–b. The figure legends "Imposing u" and "Imposing $\dot{u}$" denote the results obtained with formulations (7) and (12), respectively. The obtained convergence rates, in both cases, allow to conclude that the proposed Global–Local schemes perform well, indeed they perform a little bit better than FEM. This observation can be explained by the fact that in the Global–Local schemes the local domain is able to capture much better the steep gradients around the heat source than FEM, because the local domain moves following the heat source.

4.1.3. Test 3: global and local domains with different mesh sizes

In the previous tests, the numerical performance of the proposed Global–Local schemes was studied using the same mesh size for the global and local domains. However, the aim is to use a coarse mesh for the global domain and a fine mesh for the domain describing local features. In what follows, this issue is studied. For that purpose, the same one and two dimensional problems of the previous test are solved, but now using for the global domain a mesh size 10 times larger than the mesh size of the local domain.

The attained convergence in space can be observed in Fig. 6a–b. In addition, the solution at the end of the corresponding time interval and the temperature evolution at a material point are shown in Fig. 7a–d. A mesh size equal to $\sigma/4$ is used for the local domain in the one-dimensional study, whereas, for the two-dimensional case, a mesh size equal to $\sigma/\sqrt{8}$ is used for the local domain. As it can be appreciated from the results, the Global–Local schemes perform quite well even when the global domain has a mesh size much larger than that of the local domain.

4.1.4. Imposition of the material time derivative of temperature as compatibility constraint

Two alternatives were proposed as compatibility constraints. In the first one, denoted in the figures as "Imposing u", the compatibility constraint on the interface Γ consists in equalling the temperatures of the global and local domains, that is $u^c = u^f$. In the second alternative, the interface Γ is split into two non-overlapping portions, $\hat{\Gamma}$ and $\Gamma - \hat{\Gamma}$,

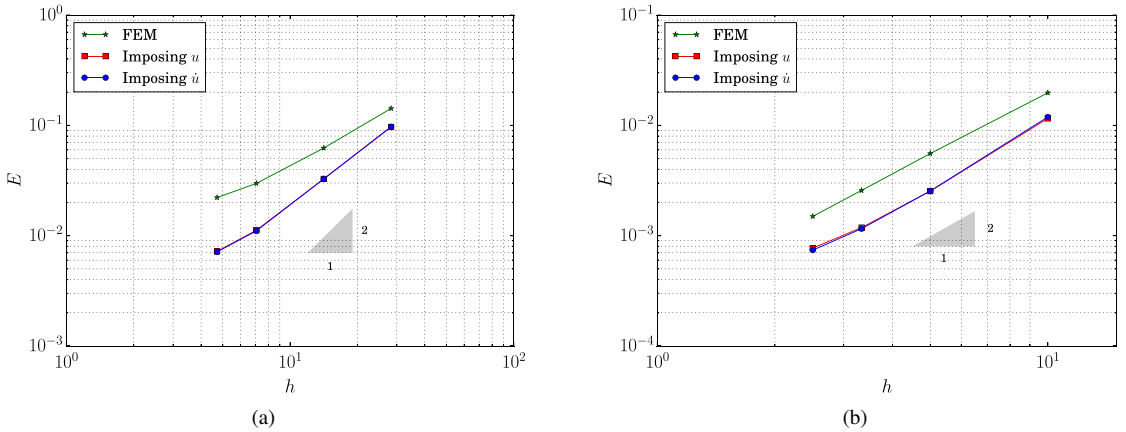

Fig. 5. Results obtained using equal mesh sizes for the global and local domains. (a) Convergence for the 2D case. (b) Convergence for the 1D case.

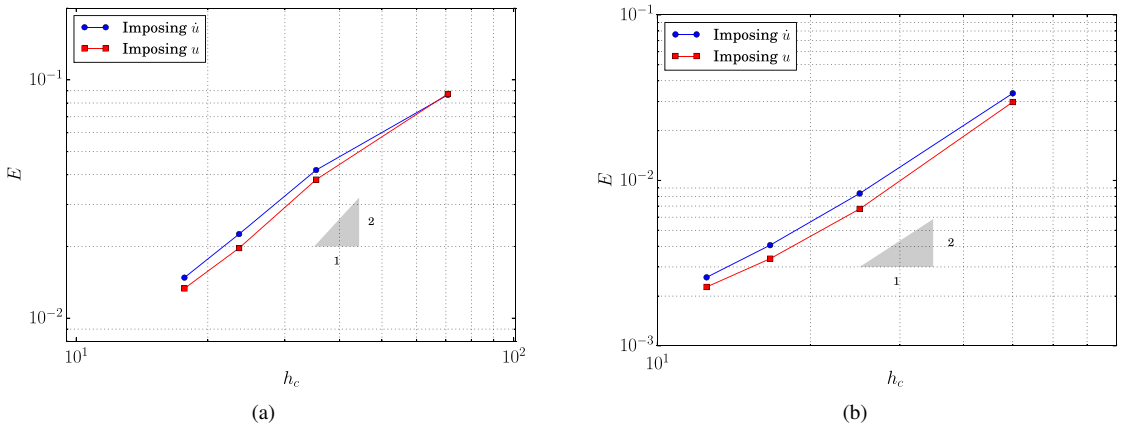

Fig. 6. Results obtained using a mesh size for the global domain 10 times bigger than the mesh size for the local domain. (a) Convergence for the 2D case. (b) Convergence for the 1D case.

where $\hat{\Gamma}$ is the portion of Γ in which $v \cdot n < 0$, with n as the outward normal of Γ. Then, the (material) temperature time derivative is imposed as compatibility constraint on $\hat{\Gamma}$, whereas temperature is imposed as compatibility constraint on $\Gamma - \hat{\Gamma}$. The numerical experiments presented next can help to understand the nature of these constraints.

First, it should be kept in mind that the projection of u^c_{n-1} to the mesh configuration at time step t_n is performed by collocation. The effect of the adopted compatibility constraint on the quality of the obtained solution can be appreciated in Fig. 8a–b. It can be observed in the zoomed regions, that the computed solution gets a nonphysical curvature when imposing the temperature as compatibility constraint. On the other hand, when imposing compatibility of the (material) time derivatives of temperature, this spurious curvature does not take place. Although this behaviour occurs locally and does not affect considerably the global error, it can be seen that imposing compatibility of the material time derivative of temperature leads to better results.

The reason why imposing compatibility of the solution on the temperature field leads locally to nonphysical solutions, is based on the observation that the local and global domains differ considerably in their resolutions and, therefore, in the behaviour that they can capture. Additionally, the involved projection to build u^c_{n-1} is performed by collocation. Then, at the boundary of the local and global domains, the rich local solution must adapt itself very rapidly to meet compatibility with the poor solution represented by the global domain. When high temperature gradients develop in the vicinity of the boundary, the imposition of the compatibility on the temperature leads to a locally

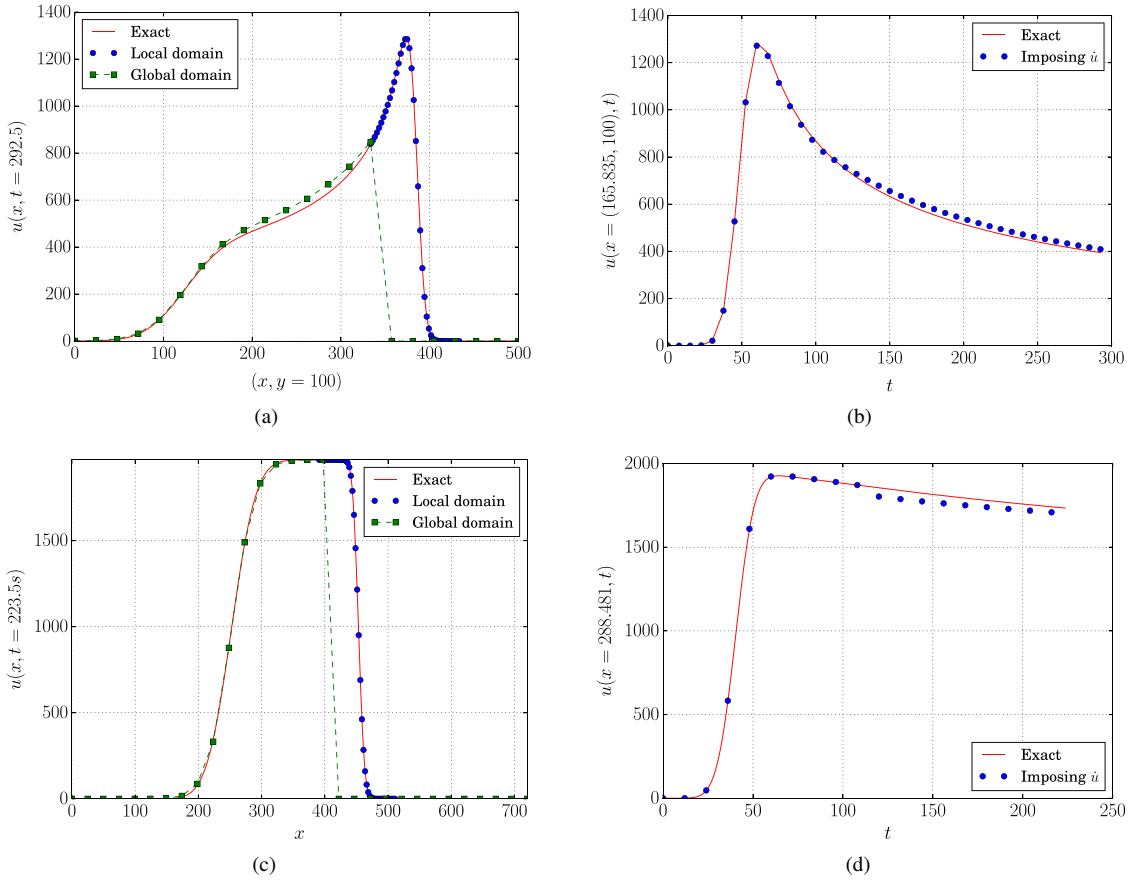

Fig. 7. Results obtained at the end of the corresponding time interval, for mesh sizes of the local domain equal to $\sigma/4$ and $\sigma/\sqrt{8}$ for the one and two dimensional cases, respectively. (a) Temperature distribution 2D test. (b) Temperature evolution 2D test. (c) Temperature distribution 1D test. (d) Temperature evolution 1D test.

nonphysical gradient. By assuming that the solution varies rapidly only inside the local domain, we may consider that temperature variation on the boundary between the local and global domains is small. Therefore, when imposing compatibility of the material time derivative of the temperature field, it is expected that both domains will be able to represent the variation of that field on the boundary with the same degree of resolution and thus avoiding nonphysical artifacts.

It should also be noted that compatibility of the material time derivative of temperature is imposed only on the part of the boundary satisfying $v \cdot n < 0$. On the other portion of the boundary, compatibility is imposed on the temperature field and not on the derivative of temperature. It is remarked that a fixation, *i.e.* imposing equality of temperature, must be given at some points in order to avoid magnifying any source of error, for instance those coming from the projection by collocation of u^c_{n-1} to the mesh configuration at time step t_n.

4.2. Numerical performance evaluation of the Reduced Order Model

The problem shown in Fig. 9a is run as training problem. The conductivity of the material is 2 and the volumetric heat capacity is 1. The σ parameter for the heat source is equal to 5 and $Q_m = 100$, a time increment of $\Delta t = 5$ is used and the trajectory followed by the heat source is modelled using 28 time steps for each trajectory segment. The global domain is discretised using 20 divisions in the x and y directions. The local domain has a size of 60×60 with a discretisation of 74 divisions for the x and y directions. The moving local domain is located with its centre

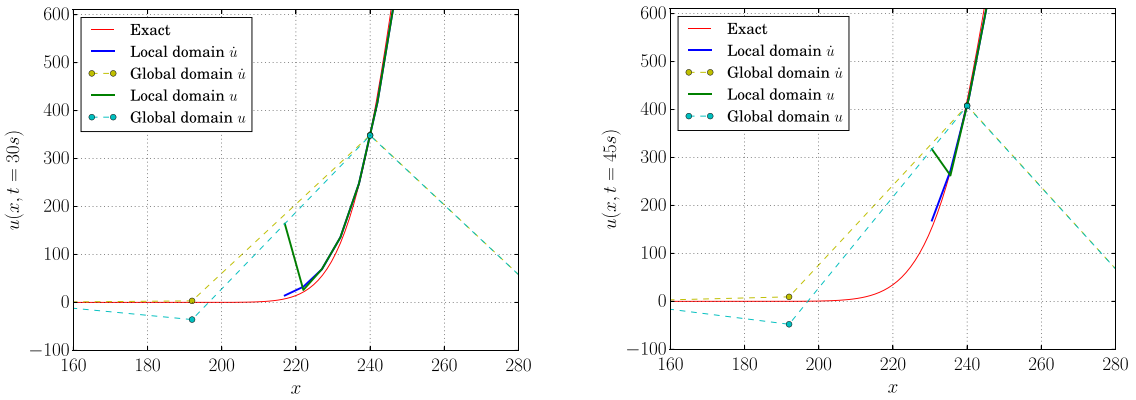

Fig. 8. Results obtained for a 1D test at two time instants using for the local domain a mesh size of $\sigma/4$ and for the global domain a mesh size 10 times bigger with a time increment of $\Delta t = 0.15$ s. In the zoomed regions it can be observed that a nonphysical curvature is adopted by the solution obtained when imposing the temperature as compatibility constraint. On the other hand, imposing the (material) temperature variation with time as compatibility, that curvature does not take place.

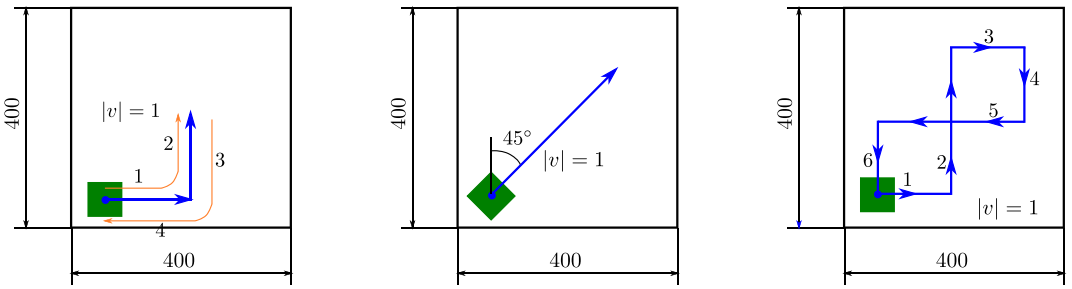

Fig. 9. In blue the trajectory to be followed by the heat source; in green the moving local domain. (a) Trajectory of the training problem, referred to as "Training". (b–c) Problems to be solved with the Reduced Order Model during the on-line stage. They are referred to as "Rotate" and "Eight", respectively. (For interpretation of the references to colour in this figure legend, the reader is referred to the web version of this article.)

coincident with the centre of the heat source. The error E_f is computed as

$$E_f = \frac{\|U - U_{ref}\|_f}{\|U_{ref}\|_f}, \tag{16}$$

where $\|\cdot\|_f$ is the Frobenius norm of $\cdot$ and U is an approximation to U_{ref}, and where both U and U_{ref} are space–time matrices. This error is computed with the involved quantities evaluated on a reference mesh with 200 divisions in the x and y directions.

The modes for the temperature field of the local domain and for the Lagrange multipliers field were computed using the described training problem. Compatibility of (material) time derivatives of temperature was imposed on the boundary $\hat{\Gamma}$. Then, the ROM given by Eq. (14) was built. In order to test the ROM performance, several problems with different heat source trajectories have been analysed, always using the same training problem. The objective was to determine if space–time dimensions show *separability* for trajectories different from those used for training. Two examples, different from the training problem, are shown in Fig. 9b–c. The only difference from the training problem is the trajectory followed by the heat source, and the other parameters were kept the same.

Fig. 10 displays the error obtained for the tested problems. In all cases the error decreases when the number of modes is incremented. However, as expected, the rate at which this error decreases is related to the similarity of the

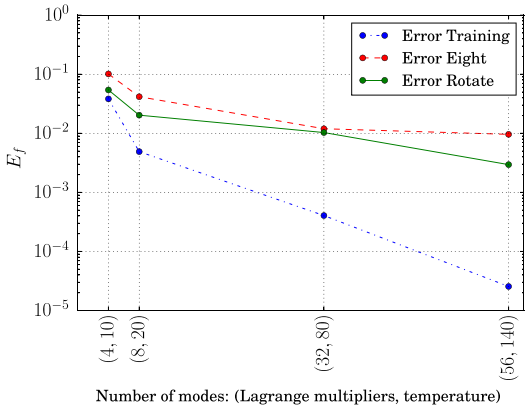

Fig. 10. Error of the developed ROM for different number of modes. In the figure the x-axis is plotted against the number of modes used for the temperature field, however the number of modes for the Lagrange multipliers is also specified.

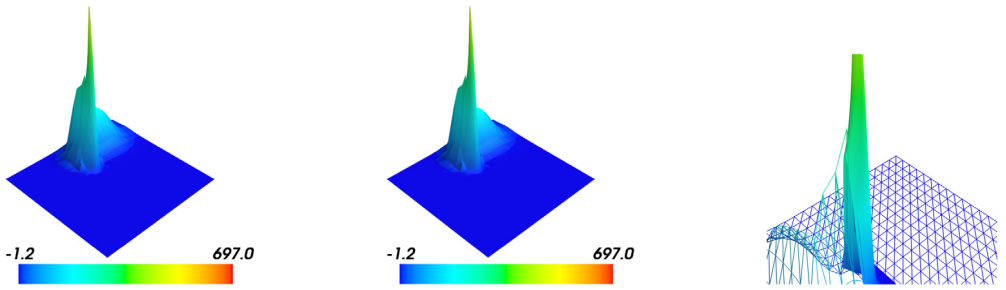

(a) HF 225 s. (b) ROM 225 s. (c) HF 225 s detail.

Fig. 11. (a–b) Comparison of the results obtained for the "Training" test using 32 modes for the Lagrange multipliers and 80 modes for the temperature field. HF denotes High Fidelity model and ROM denotes Reduced Order Model. (c) Details of the HF model in which the coarse mesh of the global domain is shown as a wire-frame overlapped to the mesh of the local domain drawn with filled triangles.

tested problem with the training one. Despite this fact, note that for a number of 20 temperature modes, the error is already below 5×10^{-2} in all cases, showing a good numerical performance.

The heat source in the training problem follows a trajectory with two segments at 90° from each other, travelled twice in a round-trip manner (Fig. 9a). The local domain does not change when the trajectory direction is modified. What changes is the velocity vector of the heat source and the portion of the boundary of the local domain in which the compatibility of the material time derivative of temperature is imposed. From the *training* point of view, it is essential to train for the different possible changes of direction of the velocity. However, in order to analyse the sensitivity of the ROM, the proposed training does not train every change of direction. More specifically, only the following changes of directions were trained: left-to-bottom, bottom-to-top and top-to-right. The temperature plot at a given time instant computed with the High Fidelity (HF) and with the ROM models (80 temperature modes and 32 Lagrange multipliers modes) can be observed in Fig. 11a–b. No difference between them can be noticed from a qualitative point of view.

One detail concerns the quality of the solution obtained with the Global–Local scheme. In Fig. 11c, a detail of the HF model is shown, in which the coarse mesh of the global domain is drawn as a wire-frame and, overlapped, the mesh of the local domain is drawn with filled triangles. Having in mind the involved coarse mesh of the global domain, from the qualitative point of view the solution looks quite good. The discontinuity observed at the interface between the global and local domains is, in part, due to the difference between the mesh sizes of the global and local domains, and due to the span of the support of the local domain which is quite small for the considered example.

In the test example of Fig. 9b, the *trained* local domain is rotated 45° and, then, the heat source follows the displayed 45° trajectory. The difficulty of this example resides in that the local domain is *cutting* the structured mesh of the global domain slantingly. It should be observed that in the training problem, the local domain cuts the mesh of

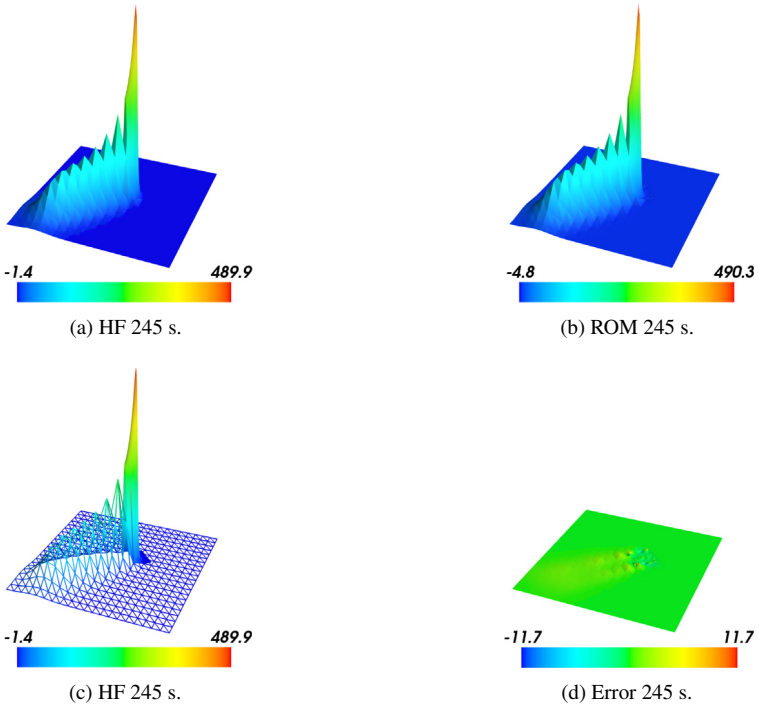

(a) HF 245 s. (b) ROM 245 s.

(c) HF 245 s. (d) Error 245 s.

Fig. 12. Comparison of the results obtained for the "Rotation" test using 32 modes for the Lagrange multipliers and 80 modes for the temperature field. HF denotes High Fidelity model and ROM denotes Reduced Order Model.

the global domain following the x and y axes. This difference introduces a complication to the ROM, mainly because of the behaviour of the Lagrange multipliers. The obtained results at a given instant can be observed in Fig. 12a–d. Note that, despite the fact that the local domain travels slantingly to the mesh of the global domain, the ROM predicts quite well the solution. Another important observation must be done concerning the behaviour of the Global–Local scheme. The peaks observed in the solution resemble symptoms of instability. However, this is not the case, and the reason for these peaks resides in the size of the coarse mesh of the global domain. Since the heat source follows a trajectory that is not aligned to any of the axes of the structured coarse mesh, it results in a poorer spatial resolution which cannot represent accurately the sharp gradient transverse to the trajectory, thus having as outcome the observed peaks.

The last tested example is the one shown in Fig. 9c. It consists in an *eight*-shaped trajectory, whose main difficulty lies in the many changes of directions that have not been trained. The obtained solutions for the HF and ROM models at several time instants are plotted in Fig. 13. At the beginning (Fig. 13a–c), the error is quite low because at this stage the problem is quite similar to the training problem. Following along the trajectory, the heat source performs a change of direction that has not been trained (Fig. 13d–f), and the observed error increments its magnitude considerably. As it was mentioned this was an expected behaviour, nonetheless it must be noted that from the qualitative point of view the HF and ROM solutions do not differ so much. Another point in the trajectory that can represent a problem is when the heat source *crosses* over a previously heated region. This can be observed in Fig. 13g–i. It can be seen that the solution looks good from the qualitative point of view, despite the fact that the error has spread further from the position of the heat source.

5. Conclusions and future work

Global–Local schemes and Reduced Order Models were investigated with the particular application to problems with steep moving gradients, such as those produced by a highly concentrated moving heat source. More specifically, the focus was placed on parabolic problems with highly concentrated moving sources such as those appearing in

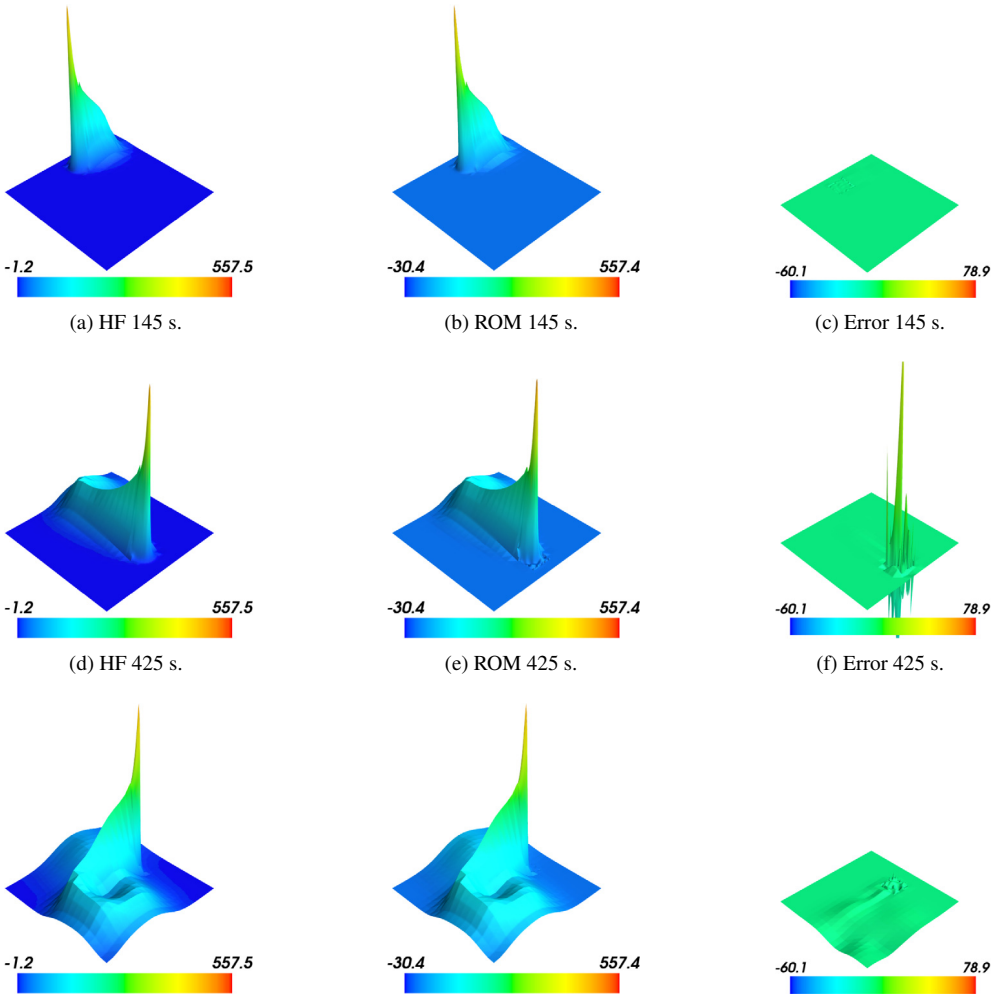

(a) HF 145 s. (b) ROM 145 s. (c) Error 145 s.

(d) HF 425 s. (e) ROM 425 s. (f) Error 425 s.

(g) HF 950 s. (h) ROM 950 s. (i) Error 950s.

Fig. 13. Comparison of the results obtained for the "Eight" test using 32 modes for the Lagrange multipliers and 80 modes for the temperature field. HF denotes High Fidelity model and ROM denotes Reduced Order Model.

selective laser melting processes. In order to exploit the local nature of the steep moving gradients, the neighbourhood of the heat source was modelled with a moving local domain which is coupled to the global domain without requiring any re-mesh and preserving the meshes of both domains during the whole simulation. Two different approaches were tested for compatibility constraint: imposing equality of temperature and imposing equality of the material time derivative of temperature in the opposite portion of the boundary to the advancing direction of the heat source. It was shown through convergence studies that both Global–Local schemes perform well.

The formulation of an *a posteriori* ROM technique based on the POD method was proposed for dealing with the dimensionality of the problem of the local domain. The evaluation tests showed that the ROM performs well. For instance, the relative error was below 5×10^{-2} when the number of temperature modes was equal to 20. We remark that, with the proposed Global–Local ROM, it was possible to successfully run problems with a trajectory different from the one used in the training phase. This is an issue very difficult to tackle with traditional ROM techniques due to the fact that the space and time dimensions do not show *separability*.

The presented Global–Local ROM methodology is in its onset. Future work needs to be carried out in many aspects. One of them is the formulation of a *Hyper*-Reduced Order Model based in the proposed ROM, to efficiently handle non-linear problems [2,20]. Other aspects concern the improvement of the introduced Global–Local schemes, such

as, for example, by further studying the involved projections, by developing a method for handling the changes of properties of the underlying material, and by allowing the deformation of the local domain. It should be observed that the last point could be of interest for solving problems with internal interfaces, as those found in fluid mechanics and phase change problems.

Acknowledgments

This work received financial support from Consejo Nacional de Investigaciones Científicas y Técnicas (PIP 112-201101- 01105), Agencia Nacional de Promoción Científica y Tecnológica (PICT 2013-2894), Universidad Nacional del Litoral (CAI+D 2011 50320140300016LI).

References

[1] M. Hamide, E. Massoni, M. Bellet, Adaptive mesh technique for thermalmetallurgical numerical simulation of arc welding processes, Internat. J. Numer. Methods Engrg. 73 (5) (2008) 624–641.
[2] A. Cosimo, A. Cardona, S. Idelsohn, Improving the k-compressibility of hyper reduced order models with moving sources: applications to welding and phase change problems, Comput. Methods Appl. Mech. Engrg. 274 (2014) 237–263.
[3] P.-E. Allier, L. Chamoin, P. Ladevèze, Proper generalized decomposition computational methods on a benchmark problem: introducing a new strategy based on constitutive relation error minimization, Adv. Model. Simul. Eng. Sci. 2 (1) (2015) 17.
[4] D. Canales, A. Leygue, F. Chinesta, D. Gonzlez, E. Cueto, E. Feulvarch, J.-M. Bergheau, A. Huerta, Vademecum-based GFEM (V-GFEM): optimal enrichment for transient problems, Internat. J. Numer. Methods Engrg. 108 (9) (2016) 971–989.
[5] P. O'Hara, C. Duarte, T. Eason, Generalized finite element analysis of three-dimensional heat transfer problems exhibiting sharp thermal gradients, Comput. Methods Appl. Mech. Engrg. 198 (2126) (2009) 1857–1871.
[6] P. O'Hara, C. Duarte, T. Eason, Transient analysis of sharp thermal gradients using coarse finite element meshes, Comput. Methods Appl. Mech. Engrg. 200 (58) (2011) 812–829.
[7] G. Houzeaux, R. Codina, A chimera method based on a dirichlet / Neumann (Robin) coupling for the Navier-Stokes equations, Comput. Methods Appl. Mech. Engrg. 192 (3132) (2003) 3343–3377.
[8] A. Lozinski, O. Pironneau, Numerical zoom for advection diffusion problems with localized multiscales, Numer. Methods Partial Differential Equations 27 (1) (2011) 197–207.
[9] H.B. Dhia, G. Rateau, The Arlequin method as a flexible engineering design tool, Internat. J. Numer. Methods Engrg. 62 (11) (2005) 1442–1462.
[10] A. Christophe, Y.L. Bihan, F. Rapetti, A mortar element approach on overlapping non-nested grids: Application to eddy current non-destructive testing, Appl. Math. Comput. 267 (2015) 71–82.
[11] A. Christophe, L. Santandrea, F. Rapetti, G. Krebs, Y. Le Bihan, An overlapping nonmatching grid mortar element method for Maxwell's equations, IEEE Trans. Magn. 50 (2) (2014) 409–412.
[12] K. Zeng, D. Pal, N. Patilal, B. Stucker, A new dynamic mesh method applied to the simulation of selective laser melting, in: Solid Freeform Fabrication Symp., Austin, TX, USA, 2013.
[13] L. Gendre, O. Allix, P. Gosselet, F. Comte, Non-intrusive and exact global/local techniques for structural problems with local plasticity, Comput. Mech. 44 (2) (2009) 233–245.
[14] A. Popp, Mortar Methods for Computational Contact Mechanics and General Interface Problems, Ph.D. thesis, Technical University of Munich, 2012.
[15] F.B. Belgacem, The Mortar finite element method with Lagrange multipliers, Numer. Math. 84 (2) (1999) 173–197.
[16] D. Dureisseix, H. Bavestrello, Information transfer between incompatible finite element meshes: Application to coupled thermo-viscoelasticity, Comput. Methods Appl. Mech. Engrg. 195 (44–47) (2006) 6523–6541.
[17] J. Donea, A. Huerta, Finite Element Methods for Flow Problems, in: Finite Element Methods for Flow Problems, John Wiley & Sons, 2003.
[18] A. Nouy, A priori model reduction through Proper Generalized Decomposition for solving time-dependent partial differential equations, Comput. Methods Appl. Mech. Engrg. 199 (23–24) (2010) 1603–1626.
[19] D. Ryckelynck, A priori hyperreduction method: an adaptive approach, J. Comput. Phys. 202 (1) (2005) 346–366.
[20] J.A. Hernandez, Dimensional hyper-reduction of parameterized , nonlinear finite element models via empirical cubature, Vol. 313, 2016, pp. 687–722.
[21] L. Sirovich, Turbulence and the dynamics of coherent structures. I - Coherent structures. II - Symmetries and transformations. III - Dynamics and scaling, Quart. Appl. Math. 45 (1987) 561–571.
[22] G. Strang, The fundamental theorem of linear algebra, Amer. Math. Monthly 100 (9) (1993) 848–855.
[23] A. Cosimo, A. Cardona, S. Idelsohn, General treatment of essential boundary conditions in reduced order models for non-linear problems, Adv. Model. and Simul. in Eng. Sci. 3 (1) (2016).
[24] K. Carlberg, C. Bou-Mosleh, C. Farhat, Efficient non-linear model reduction via a least-squares PetrovGalerkin projection and compressive tensor approximations, Internat. J. Numer. Methods Engrg. 86 (2) (2011) 155–181.
[25] J. O'Rourke, Computational Geometry in C, second ed, Cambridge University Press, New York, NY, USA, 1998.
[26] K. Cole, J. Beck, A. Haji-Sheikh, B. Litkouhi, Heat Conduction Using Green's Functions, second Edition, in: Series in Computational Methods and Physical Processes in Mechanics and Thermal Sciences, CRC Press, 2010.